Autoionizing resonances in electron-impact excitation of oxygenlike selenium

K. J. Reed, M. H. Chen, and A. U. Hazi
High Temperature Physics Division, Lawrence Livermore National Laboratory, Livermore, California 94550
(Received 5 April 1988)

We have investigated the contributions of doubly excited, autoionizing resonances to the rate coefficients for electron-impact excitation of the $n=2$ to $n=2$ transitions in oxygenlike selenium. The cross sections for direct excitation were calculated using a relativistic distorted-wave approximation. The detailed Auger and radiative rates required for evaluating the resonance contributions were calculated using a multiconfigurational Dirac-Fock model. The largest effect is on the electric-dipole-forbidden transitions. For some $J=0$ to $J=0$ transitions involving two-electron excitations, the resonances enhance the collisional excitation rates by factors up to 10^4 at electron temperatures relevant for laboratory plasmas.

I. INTRODUCTION

Electron-impact excitation of positive ions is an important process occurring in astrophysical plasmas and in plasmas produced in laboratory experiments. Since electron-collisional rate coefficients for large numbers of transitions are needed for codes used to model these plasmas, there is heavy reliance upon approximations which allow for rapid computation of the required cross sections.[1] While the distorted-wave approximation and other weak coupling methods provide relatively rapid tools for calculating these cross sections, they neglect the contributions of indirect processes involving doubly excited autoionizing states.

In earlier studies of electron collisions with light positive ions it was found that autoionizing resonances can significantly increase the calculated rates for excitation of some transitions,[1] and more recently similar effects have been noted in studies of highly charged ions.[2–10] For example, such resonances enhanced the calculated excitation rates of the $2p^6 \rightarrow 2p^5 3s$ transitions in neonlike ions[4,5,8–10] by factors of 2–6. Similar enhancements were observed for some electric-dipole-forbidden, $\Delta n=0$, transitions in fluorinelike[6] and berylliumlike ions.[7] In this paper we report results of calculations of resonance contributions to the electron-collisional excitation rates for transitions between the $n=2$ states of oxygenlike selenium.

Oxygenlike ions are important constituents of plasmas produced in magnetic fusion experiments, and in laser produced plasmas. Lasing in the soft x-ray regime has been observed from neonlike ions created by laser heating of selenium and other targets.[11] Through recombination processes, charge states with partially filled L shells, e.g., oxygenlike or fluorinelike, can affect the population of neonlike ions. Furthermore, radiation emitted from excited states of these ions can provide electron-temperature and density diagnostic information about the plasmas.[12,13]

The $n=2$ complex of oxygenlike selenium consists of ten levels, which are connected by a variety of types of transitions. In a previous paper[6] we discussed the Z dependence of resonance enhancement for the three $n=2$ to $n=2$ transitions in the fluorine isoelectronic sequence. In this work, we consider a single ionic species, but we study the importance of resonance contributions for a greater variety of transitions. In general, we find that the more "forbidden" the transition is in the sense of the electric multipole expansion, the greater the resonance enhancement of the excitation rate coefficients. For example, the rate coefficients of the strong electric-dipole transitions are hardly affected, while those for the electric-quadrupole transitions are increased by factors of up to 4, and those for the most forbidden $j=0$ to $j=0$ transitions are enhanced by *four orders of magnitude.*

II. CALCULATIONAL PROCEDURES

The resonances are produced when an oxygenlike ion is excited by a free electron which is simultaneously captured forming a doubly excited fluorinelike ion. The doubly excited ion may stabilize by emission of a photon, and in this case the event is a contribution to dielectronic recombination. If the doubly excited fluorinelike ion autoionizes, the resulting oxygenlike ion may be left in a singly excited state and the event is a resonance contribution to the electron-impact excitation of the oxygenlike ion. We consider two-step processes of the following types:

$$2s^p 2p_{1/2}^q 2p_{3/2}^r + e \rightarrow 2s^{p'} 2p_{1/2}^{q'} 2p_{3/2}^{r'} nljn'l'j' \rightarrow 2s^{p''} 2p_{1/2}^{q''} 2p_{3/2}^{r''} + e \ , \quad (1)$$

where

$$p'+q'+r'=5$$

and

$$p+q+r=p''+q''+r''=6 \ .$$

For $n=2$ in Eq. (1), the intermediate state can autoionize via a Coster-Kronig transition in which there is no change in principal quantum number of one of the active electrons. In this case, we include all intermediate states

with $n' \leq 15$. For intermediate states with $n=3$, the Auger rates vary as $(n')^{-3}$ and the resonance contribution scales as $(n')^{-6}$. We include values of n' up to $n'=6$ for these states.

The nonresonant background cross sections were calculated using a relativistic distorted-wave approximation.[14] Relativistic multiconfiguration target wave functions were computed using a Dirac-Fock atomic structure code which is part of an atomic physics package YODA developed by Hagelstein.[14] We included the ten states listed in Table I plus all the configurations formed by promotion of an $n=2$ electron to an $n=3$ orbital. Partial waves up to $l=12$ were sufficient to converge the cross section at all energies up to ten times threshold for the electric-dipole-forbidden transitions. For the dipole-allowed transitions, partial waves up to $l=70$ were computed. We assume a Maxwellian distribution of the electrons in the plasma for calculating the rate coefficients.

The resonance contribution was calculated using a procedure given by Cowan.[15] The scattering amplitude is separated into resonant and nonresonant parts using a projection-operator formalism. The interference between the two parts is neglected and the resonance contribution is calculated in the isolated-resonance approximation. Radiative decay of the autoionizing states to singly excited states is included, but radiative cascades among autoionizing states are ignored.

The rate coefficient $C_{id}^{\rm cap}$ for capture of a free electron can be obtained from the inverse Auger process by detailed balance,

$$C_{id}^{\rm cap}=(2g_i)^{-1}\left[\frac{4\pi R}{kT}\right]^{3/2} a_0^3 \exp(-E_{di}/kT) g_d A_{di}^a \ . \quad (2)$$

Here i represents the initial state of the O-like ion and d represents the doubly excited F-like state formed in the capture process. g_i and g_d are the statistical weights of the states i and d, respectively, and R is the Rydberg energy. A_{di}^a and E_{di} are the autoionization rate and the excitation energy for the transition d to i.

The branching ratio B_{df}^a for autoionization from the doubly excited state d of the F-like ion to some final (excited) state f of the O-like ion is given by

$$B_{df}^a=\frac{A_{df}^a}{\Gamma_a(d)+\Gamma_r(d)} \ , \quad (3)$$

where

$$\Gamma_a(d)=\sum_m A_{dm}^a, \quad \Gamma_r(d)=\sum_n A_{dn}^r \ . \quad (4)$$

In Eq. (4), m represents any of the possible final states of the O-like ion accessible by Auger decay of the doubly excited state d, n represents any of the possible states of the F-like ion accessible by radiative decay of the same state, and A_{dn}^r is the radiative rate for the transition $d \rightarrow n$.

The total resonance contribution to the excitation rate from state i to state f of the O-like ion is obtained by multiplying $C_{id}^{\rm cap}$ by B_{df}^a and summing over all intermediate states d,

$$C_{if}^{\rm res}=\sum_d C_{id}^{\rm cap} B_{df}^a \ . \quad (5)$$

In the present work, the detailed Auger and radiative rates and the energies of the autoionizing states were calculated using the multiconfiguration Dirac-Fock model (MCDF).[16,17] The energy levels and wave functions for the intermediate states were calculated explicitly in intermediate coupling, including configuration interaction within the same complex by using the MCDF model in the average-level scheme (AL).[17] Separate MCDF-AL calculations were performed for the O-like and F-like configurations.

This method of treating the resonance contributions is appropriate for highly charged ions where relativistic effects and radiative channels become important, and where the widths of the resonances are small compared to the energy spacings between neighboring resonances. The close-coupling approximation can properly account

TABLE I. Energy levels for the $n=2$ complex of oxygenlike selenium.

State	Configuration	J	Energy (eV)	LSJ
1	$1s^2 2s^2 2p_{1/2}^2 2p_{3/2}^2$	2	0.00	$^3P_2$
2	$1s^2 2s^2 2p_{1/2}^2 2p_{3/2}^2$	0	17.95	$^3P_0$
3	$1s^2 2s^2 2p_{1/2}^1 2p_{3/2}^3$	1	40.08	$^3P_1$
4	$1s^2 2s^2 2p_{1/2}^1 2p_{3/2}^3$	2	52.38	$^1D_2$
5	$1s^2 2s^2 2p_{3/2}^4$	0	100.87	$^1S_0$
6	$1s^2 2s^1 2p_{1/2}^2 2p_{3/2}^3$	2	185.71	$^3P_2$
7	$1s^2 2s^1 2p_{1/2}^2 2p_{3/2}^3$	1	205.89	$^3P_1$
8	$1s^2 2s^1 2p_{1/2}^1 2p_{3/2}^4$	0	229.81	$^3P_0$
9	$1s^2 2s^1 2p_{1/2}^1 2p_{3/2}^4$	1	261.34	$^1P_1$
10	$1s^2 2p_{1/2}^2 2p_{3/2}^4$	0	423.17	$^1S_0$

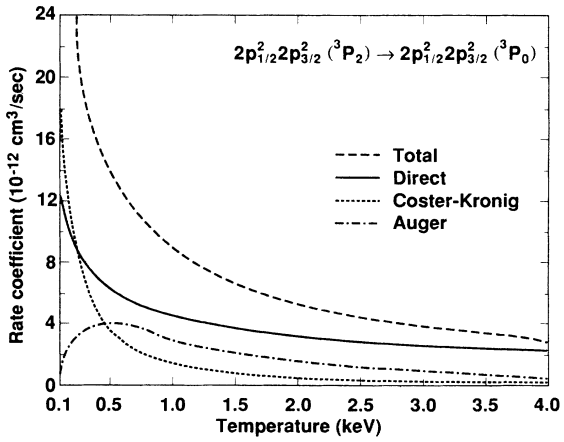

FIG. 1. Excitation rate coefficients for $2s^2 2p_{1/2}^2 2p_{3/2}^2 (^3P_2) \rightarrow 2s^2 2p_{1/2}^2 2p_{3/2}^2 (^3P_0)$ transition.

for interference between the resonant and nonresonant contributions to the scattering amplitude, but current computer codes employing this approximation are limited to the use of nonrelativistic target orbitals and do not include the radiative decay of the doubly excited states.[1,8]

III. RESULTS AND DISCUSSION

In Figs. 1–4 we compare the direct electron-collisional rates and the resonance contributions for a few selected transitions in oxygenlike selenium. The resonance contributions due to Coster-Kronig transitions are shown separately from those due to Auger transitions in Figs. 1 and 2. At low temperatures, the resonance excitation is dominated by the Coster-Kronig process. The Coster-Kronig contribution to the rates usually peaks below 100 eV and drops rapidly with increasing electron temperature to some nearly constant value. The Auger contribution peaks near 500 eV and drops less precipitously with increasing electron temperature.

In Fig. 5 we show the Coster-Kronig contributions for transitions from level 2 ($2s^2 2p_{1/2}^2 2p_{3/2}^2$, $J=0$) to different final states. These contributions diminish as the transition energy increases because the Coster-Kronig mechanism becomes energetically possible only for much higher values of n' [see Eq. (1)].

In Table II, we show the direct electron-impact excitation rate coefficients and the resonance contributions for all of the transitions among the $n=2$ levels of oxygenlike selenium. The effect of the resonances on the electric-dipole-allowed transitions is less than 10%, and in some cases it is only 1%. For the electric-quadrupole transitions, the resonance contributions are sometimes approximately equal to the direct excitation rate coefficients. The direct rates for some of the quadrupole transitions are already quite large. For example, at 500 eV, the direct rate is 1.78×10^{-11} cm^3/sec for the 1-4 transition

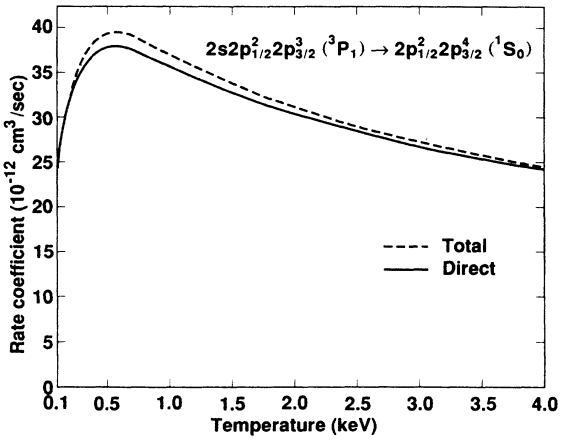

FIG. 3. Excitation rate coefficients for $2s^1 2p_{1/2}^2 2p_{3/2}^3 (^3P_1) \rightarrow 2p_{1/2}^2 2p_{3/2}^4 (^1S_0)$ transition.

(from level 1 to level 4), and 2.52×10^{-11} cm^3/sec for the 3-4 transition. At the same temperature, the resonance contributions to these transitions are 2.13×10^{-11} cm^3/sec and 2.69×10^{-11} cm^3/sec, respectively. In absolute terms, these are among the largest resonance contributions and their effect is to more than double the collisional excitation rate coefficients for these transitions.

The transitions which involve transfer of two electrons proceed only through configuration interaction and spin-orbit mixing, and the rate coefficients for direct excitation of these transitions are generally small. The effect of the resonances on some of these transitions is considerable. For example, the 1-5 transition involves transfer of two electrons from the $2p_{1/2}$ orbital to the $2p_{3/2}$ orbital, and has a direct rate of only 2.35×10^{-13} cm^3/sec at 500 eV. As Fig. 2 shows, the resonance contribution enhances the

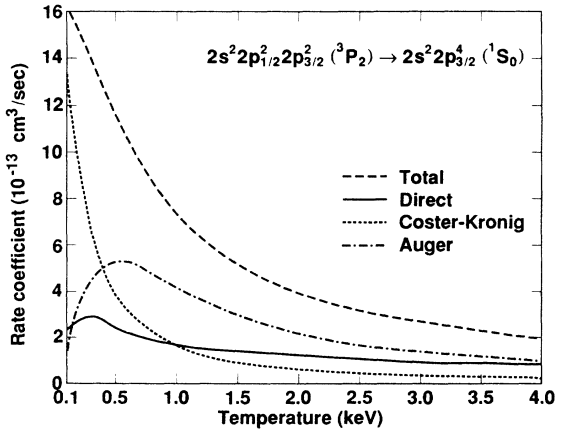

FIG. 2. Excitation rate coefficients for $2s^2 2p_{1/2}^2 2p_{3/2}^2 (^3P_2) \rightarrow 2s^2 2p_{3/2}^4 (^1S_0)$ transition.

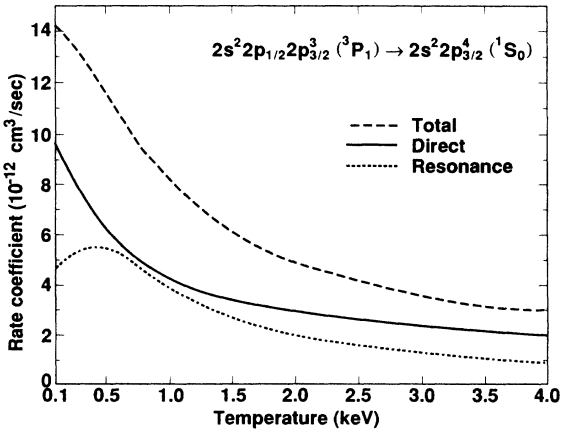

FIG. 4. Excitation rate coefficients for $2s^2 2p_{1/2}^1 2p_{3/2}^3 (^3P_1) \rightarrow 2s^2 2p_{3/2}^4 (^1S_0)$ transition.

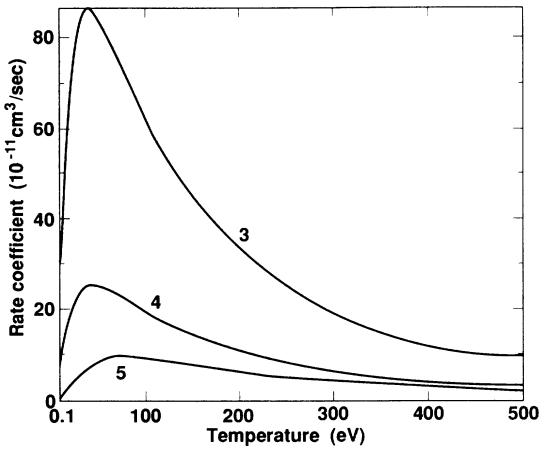

FIG. 5. Coster-Kronig contributions to excitation rate coefficients for transitions from level 2 ($2s^2 2p_{1/2}^2 2p_{3/2}^2$, $^3P_0$) to different final states. Numbers labeling the curves are the final states listed in Table I.

rate for this transition by nearly a factor of 5 at the same temperature.

The most dramatic resonance enhancement occurs for some two-electron transitions in which both the initial state and the final state have total angular momenta of zero. The rate coefficients for direct excitation of these highly forbidden transitions are extremely small, and in some cases the resonance enhancement is enormous. The 2-5 transition, for example, has a direct rate of only 1.59×10^{-16} cm^3/sec at 500 eV and the resonance contribution is nearly a factor of *30 000* times larger. Similarly, the rate for the 5-10 transition is enhanced by a factor of more than 10^3.

It is clear from the results in Table II that the $J=0\rightarrow J=0$ transitions which have negligible direct excitation rates may have sufficiently larger resonance contributions to result in total rates which are significant and comparable to rates for other transitions. Such enhancements could have important consequences for some atomic models which have been developed for studying the kinetics of level populations in hot, nonequilibrium plasmas. In particular, the absence of expected amplification of the $2p^5 3p\rightarrow 2p^5 3s$ ($J=0\rightarrow 1$) line in

TABLE II. Direct electron-impact excitation rate coefficient (D) and resonance contributions (R) in cm^3/sec. (Numbers in brackets are powers of ten.)

Transition	Electron temperature (eV) 100	500	1000	2000
1-2				
D	1.25[−11]	6.34[−12]	4.55[−12]	3.24[−12]
R	2.44[−11]	7.75[−12]	4.40[−12]	2.10[−12]
1-3				
D	2.03[−11]	1.19[−11]	8.61[−12]	6.15[−12]
R	5.21[−11]	1.94[−11]	1.13[−11]	5.44[−12]
1-4				
D	2.77[−11]	1.78[−11]	1.30[−11]	9.35[−12]
R	3.72[−11]	2.13[−11]	1.37[−11]	6.91[−12]
1-5				
D	2.73[−13]	2.35[−13]	1.68[−13]	1.16[−13]
R	1.42[−12]	9.19[−13]	5.69[−13]	2.80[−13]
1-6				
D	4.11[−11]	8.90[−11]	8.04[−11]	6.57[−11]
R	1.91[−13]	5.09[−12]	4.33[−12]	2.44[−12]
1-7				
D	4.33[−11]	1.10[−10]	1.03[−10]	8.55[−11]
R	5.81[−14]	1.75[−12]	1.52[−12]	8.70[−13]
1-8				
D	8.43[−15]	2.10[−14]	1.63[−14]	1.04[−14]
R	6.70[−15]	3.10[−13]	2.75[−13]	1.58[−13]
1-9				
D	4.19[−12]	1.65[−11]	1.62[−11]	1.40[−11]
R	9.82[−15]	4.61[−13]	4.13[−13]	2.39[−13]
1-10				
D	1.86[−15]	2.33[−14]	2.42[−14]	2.02[−14]
R	1.41[−16]	1.90[−14]	2.06[−14]	1.32[−14]

TABLE II. (*Continued*).

Transition	Electron temperature (eV) 100	500	1000	2000
2-3				
R	2.87[−11]	2.00[−11]	1.44[−11]	1.02[−11]
R	6.18[−11]	2.79[−11]	1.71[−11]	8.44[−12]
2-4				
D	3.53[−11]	2.01[−11]	1.20[−11]	1.04[−11]
R	1.93[−11]	1.32[−11]	8.91[−12]	4.58[−12]
2-5				
D	1.91[−16]	1.59[−16]	1.21[−16]	8.75[−17]
R	9.53[−12]	4.58[−12]	2.83[−12]	1.42[−12]
2-6				
D	3.07[−12]	4.70[−12]	3.58[−12]	2.51[−12]
R	1.71[−13]	4.18[−12]	3.49[−12]	1.95[−12]
2-7				
D	7.94[−11]	1.75[−10]	1.60[−10]	1.32[−10]
R	1.30[−13]	3.72[−12]	3.15[−12]	1.77[−12]
2-8				
D	2.50[−14]	5.36[−14]	4.06[−14]	2.54[−14]
R	1.24[−14]	3.65[−13]	3.02[−13]	1.67[−13]
2-9				
D	2.17[−12]	7.35[−12]	7.02[−12]	5.95[−12]
R	1.69[−14]	7.09[−13]	6.26[−13]	3.60[−13]
2-10				
D	2.08[−17]	2.32[−16]	2.42[−16]	2.06[−16]
R	4.19[−16]	4.44[−14]	4.76[−14]	3.02[−14]
3-4				
D	5.25[−11]	2.52[−11]	1.79[−11]	1.27[−11]
R	4.22[−11]	2.69[−11]	1.81[−11]	9.24[−12]
3-5				
D	9.69[−12]	6.16[−12]	4.30[−12]	2.96[−12]
R	4.62[−12]	5.46[−12]	3.88[−12]	2.03[−12]
3-6				
D	6.56[−11]	1.08[−10]	9.69[−11]	8.06[−11]
R	4.35[−13]	5.19[−12]	4.16[−12]	2.27[−12]
3-7				
D	2.66[−11]	4.92[−11]	4.41[−11]	3.63[−11]
R	1.47[−13]	3.36[−12]	2.76[−12]	1.54[−12]
3-8				
D	3.21[−11]	7.20[−11]	6.67[−11]	5.64[−11]
R	2.79[−14]	8.67[−13]	7.36[−13]	4.15[−13]
3-9				
D	3.55[−12]	9.78[−12]	8.99[−12]	7.43[−12]
R	4.15[−14]	1.70[−12]	1.49[−12]	8.52[−13]
3-10				
D	2.46[−15]	1.97[−14]	1.72[−14]	1.14[−14]
R	4.25[−16]	3.91[−14]	4.05[−14]	2.53[−14]
4-5				
D	1.24[−11]	7.95[−12]	5.84[−12]	4.20[−12]
R	1.72[−11]	5.99[−12]	3.33[−12]	1.56[−12]
4-6				
D	2.78[−11]	4.10[−11]	3.62[−11]	2.97[−11]
R	1.04[−12]	4.71[−12]	3.82[−12]	2.11[−12]

TABLE II. (*Continued*).

Transition	Electron temperature (eV) 100	500	1000	2000
4-7				
D	4.67[−12]	7.70[−12]	6.72[−12]	5.41[−12]
R	2.24[−13]	2.03[−12]	1.67[−12]	9.33[−13]
4-8				
D	5.14[−13]	8.44[−13]	6.25[−13]	3.91[−13]
R	1.82[−14]	5.49[−13]	4.60[−13]	2.58[−13]
4-9				
D	6.36[−11]	1.68[−10]	1.61[−10]	1.40[−10]
R	6.19[−14]	2.26[−12]	1.94[−12]	1.10[−12]
4-10				
D	8.12[−15]	7.54[−14]	8.17[−14]	7.46[−14]
R	4.27[−16]	2.99[−14]	2.92[−14]	1.77[−14]
5-6				
D	7.15[−13]	5.72[−13]	4.09[−13]	2.83[−13]
R	2.45[−12]	5.04[−12]	3.51[−12]	1.79[−12]
5-7				
D	3.82[−12]	4.35[−12]	3.62[−12]	2.82[−13]
R	6.41[−14]	3.42[−12]	2.58[−12]	1.37[−12]
5-8				
D	1.78[−12]	1.99[−12]	1.40[−12]	8.46[−13]
R	5.56[−14]	1.27[−12]	1.04[−12]	5.73[−13]
5-9				
D	8.07[−11]	1.44[−10]	1.29[−10]	1.05[−10]
R	2.22[−13]	7.26[−12]	6.17[−12]	3.47[−12]
5-10				
D	1.30[−17]	7.37[−17]	7.00[−17]	5.67[−17]
R	1.67[−15]	1.04[−13]	1.03[−13]	6.27[−14]
6-7				
D	3.15[−11]	1.59[−11]	1.14[−11]	8.08[−12]
R	3.56[−12]	1.52[−11]	1.12[−11]	5.93[−12]
6-8				
D	6.08[−12]	3.72[−12]	2.70[−12]	1.93[−12]
R	2.92[−13]	3.03[−12]	2.26[−12]	1.18[−12]
6-9				
D	9.25[−12]	6.68[−12]	4.71[−12]	3.23[−12]
R	2.02[−12]	8.12[−12]	6.18[−12]	3.31[−12]
6-10				
D	5.02[−13]	1.33[−12]	8.21[−13]	6.71[−13]
R	2.21[−14]	1.17[−12]	1.05[−12]	6.11[−13]
7-8				
D	1.66[−11]	8.45[−12]	6.01[−12]	4.26[−12]
R	8.08[−13]	7.14[−12]	5.26[−12]	2.76[−12]
7-9				
D	3.52[−11]	6.67[−11]	4.27[−12]	2.83[−12]
R	3.64[−11]	2.21[−11]	1.44[−11]	7.24[−12]
7-10				
D	1.36[−11]	3.77[−11]	3.56[−11]	3.03[−11]
R	3.30[−14]	1.48[−12]	1.32[−12]	7.62[−13]
8-9				
D	2.22[−11]	1.17[−11]	8.29[−12]	5.85[−12]
R	4.21[−12]	2.45[−11]	1.84[−11]	9.73[−12]

TABLE II. (*Continued*).

Transition	Electron temperature (eV) 100	500	1000	2000
8-10				
D	7.51[−13]	1.40[−12]	1.05[−12]	6.63[−13]
R	3.83[−14]	1.67[−12]	1.47[−12]	8.40[−13]
9-10				
D	1.27[−10]	2.30[−10]	2.06[−10]	1.69[−10]
R	8.73[−14]	2.43[−12]	2.01[−12]	1.12[−12]

neonlike soft x-ray lasers has been an outstanding puzzle.[11] There has been speculation that an overestimation of the gain for this transition could result from some unexplained error in the calculated $2p^6 \rightarrow 2p^5 3p$ cross section used in the atomic models. But comparisons of cross sections from three different distorted-wave calculations[14,18,19] and a more recent close-coupling calculation[8] show reasonably good agreement for the strong $2p$-$3p$ and $2p$-$3d$ excitations, including the questionable $2p^6\,{}^1S_0$-$2p^5 3p\,{}^1S_0$ transition, in neonlike ions. In addition, some of these cross sections have now been measured[20] for Ba^{46+}, and the experimental results have not identified any major discrepancy with theory.[21] On the other hand, the $n=3$ complex of neonlike ions consists of a number of states separated by relatively small energy differences, similar to the $n=2$ complex of oxygenlike ions, and we expect that autoionizing resonances will significantly affect some of the rates for collisional mixing among these $n=3$ states. Including resonantly enhanced collision rates for highly forbidden transitions in the atomic models describing the $n=3$ complex of neonlike ions could affect the populations of some of these excited states and thereby modify the calculated gains for $2p^5 3p$-$2p^5 3s$ lasing transitions. Explicit calculations of resonance contributions to collisional rate coefficients for $n=3$ to $n=3$ transitions in neonlike selenium are currently in progress.[22]

IV. CONCLUSION

We have studied the effects of autoionizing resonances on the rate coefficients for electron-impact excitation of the transitions among the $n=2$ states of oxygenlike selenium. The contributions from these resonances increase the rate coefficients for some of the electric-quadrupole-allowed transitions by a factor of 4. For some of the forbidden transitions involving excitation of two electrons, the resonance-enhanced rate coefficients are greater than those for direct excitation by a factor of 5 or more. The most dramatic resonance enhancements are found for some of the highly forbidden $J=0 \rightarrow J=0$ transitions, where the rate coefficients are increased by factors of 10^4. As a result, transitions which have nearly negligible rate coefficients for direct excitation can have total rate coefficients comparable to those for other moderately strong transitions. Including these effects in plasma models could significantly affect the results for excited-state populations which have been obtained with models that do not account for the resonance enhancement of electron-collisional excitation rates.

ACKNOWLEDGMENTS

We thank P. L. Hagelstein and R. Jung for useful discussions and assistance with the distorted-wave collision code. This work was performed under the auspices of the U.S. Department of Energy by the Lawrence Livermore National Laboratory under Contract No. W-7405-ENG-48.

[1] R. J. W. Henry, Phys. Rep. **68**, 1 (1981).
[2] A. K. Pradhan, D. W. Norcross, and D. G. Hummer, Phys. Rev. A **23**, 619 (1981); A. K. Pradhan, *ibid.* **28**, 2113 (1983).
[3] R. E. H. Clark, A. L. Merts, J. B. Mann, and L. A. Collins, Phys. Rev. A **27**, 1812 (1983).
[4] K. J. Reed and A. Hazi, in Proceedings and Abstracts of the Eighth International Conference on Atomic Physics, Götenborg, 1982, edited by I. Lindgren, A. Rosen, and S. Svanberg (unpublished), p. 76.
[5] M. S. Pindzola, D. C. Griffin, and C. Bottcher, Phys. Rev. A **32**, 822 (1985).
[6] K. J. Reed, M. H. Chen, and A. U. Hazi, Phys. Rev. A **36**, 3117 (1987).
[7] M. H. Chen and B. Crasemann, Phys. Rev. A **37**, 2886 (1988).
[8] G. P. Grupta, K. A. Berrington, and A. E. Kingston, J. Phys. B **20**, L637 (1987).
[9] B. W. Smith, J. C. Raymond, J. B. Mann, and R. D. Cowan, Astrophys. J **298**, 898 (1985).
[10] G. Omar and Y. Hahn, Phys. Rev. A **37**, 1983 (1988).
[11] M. D. Rosen *et al.*, Phys. Rev. Lett. **54**, 106 (1985); D. L. Matthews *et al.*, *ibid.* **54**, 110 (1985); M. D. Rosen *et al.*, *ibid.* **59**, 2283 (1987).
[12] V. Feldman and G. A. Doschek, J. Opt. Soc. Am. **67**, 726 (1977).

[13]Y. T. Lee and K. J. Reed, J. Quant. Spectrosc. Radiat. Transfer **39**, 57 (1988).
[14]P. L. Hagelstein and R. K. Jung, At. Data Nucl. Data Tables **37**, 121 (1987).
[15]R. D. Cowan, J. Phys. B **13**, 1471 (1980).
[16]I. P. Grant *et al.*, Comput. Phys. Commun. **21**, 207 (1980).
[17]M. H. Chen, Phys. Rev. A **31**, 1449 (1985).
[18]K. J. Reed and A. U. Hazi (unpublished).
[19]W. H. Goldstein and K. J. Reed, in Proceedings of Conference, Atomic Processes in Hot Plasmas, Hebrew University, Jerusalem, 1986 (unpublished), p. 37.
[20]R. E. Marrs, M. A. Levine, D. A. Knapp, and J. R. Henderson, Phys. Rev. Lett. **60**, 1715 (1988).
[21]K. J. Reed, Phys. Rev. A **37**, 1791 (1988).
[22]M. H. Chen, K. J. Reed, and A. Hazi (unpublished).